tions when a large phase-velocity ratio exists, as exemplified by the pronounced bandpass response of the inhomogeneous C section in contrast with the all-pass response of the homogeneous C section.

References

[1] S. B. Cohn, "Shielded coupled-strip transmission line," *IRE Trans. Microwave Theory Tech.*, vol. MTT-3, pp. 29–38, Oct. 1955.

[2] ——, "Characteristic impedances of broadside-coupled strip transmission lines," *IRE Trans. Microwave Theory Tech.*, vol. MTT-8, pp. 633–636, Nov. 1960.

[3] H. E. Green, "The numerical solution of some important transmission-line problems," *IEEE Trans. Microwave Theory Tech. (Special Issue on Microwave Filters)*, vol. MTT-13, pp. 676–692, Sept. 1965.

[4] M. K. Krage and G. I. Haddad, "The characteristic impedance and coupling coefficient of coupled rectangular strips in a waveguide," *IEEE Trans. Microwave Theory Tech.*, vol. MTT-16, pp. 302–307, May 1968.

[5] T. G. Bryant and J. A. Weiss, "Parameters of microstrip transmission lines and of coupled pairs of microstrip lines," *IEEE Trans. Microwave Theory Tech. (1968 Symposium Issue)*, vol. MTT-16, pp. 1021–1027, Dec. 1968.

[6] S. V. Judd, I. Whiteley, R. J. Clowes, and D. C. Rickard, "An analytical method for calculating microstrip transmission line parameters," *IEEE Trans. Microwave Theory Tech.*, vol. MTT-18, pp. 78–87, Feb. 1970.

[7] J. E. Dalley, "A strip-line directional coupler utilizing a nonhomogeneous dielectric medium," *IEEE Trans. Microwave Theory Tech.*, vol. MTT-17, pp. 706–712, Sept. 1969.

[8] G. I. Zysman and A. Matsumoto, "Properties of microwave C-sections," *IEEE Trans. Circuit Theory*, vol. CT-12, pp. 74–82, Mar. 1965.

[9] E. M. T. Jones and J. T. Bolljahn, "Coupled-strip-transmission-line filters and directional couplers," *IRE Trans. Microwave Theory Tech.*, vol. MTT-4, pp. 75–81, Apr. 1956.

[10] D. L. Gish and O. Graham, "Characteristic impedance and phase velocity of a dielectric-supported air strip transmission line with side walls," *IEEE Trans. Microwave Theory Tech.*, vol. MTT-18, pp. 131–148, Mar. 1970.

[11] R. E. Collin, *Field Theory of Guided Waves*. New York: McGraw-Hill, 1960.

[12] R. L. Ketter and S. P. Prauel, Jr., *Modern Methods of Engineering Computation*. New York: McGraw-Hill, 1969.

Computer Analysis of the Fundamental and Higher Order Modes in Single and Coupled Microstrip

DOUGLAS G. CORR AND J. BRIAN DAVIES

***Abstract*—By means of finite difference methods, dispersion curves are obtained for the fundamental and higher order hybrid modes in both single and coupled microstrip. Structures of realistic proportions are investigated by the use of a graded finite difference mesh. Variational methods are used in deriving the finite difference equations. The higher order modes are found to be similar to LSM slab line modes. A spurious nonphysical class of solutions is found to exist in this and similar formulations, the characteristics of which are described.**

Manuscript received January 5, 1972; revised March 27, 1972. This work is a portion of a dissertation submitted to the University of London, London, England, by D. G. Corr in partial fulfillment of the requirements of the Ph.D. degree. It was supported by the UK Science Research Council and the UK Ministry of Technology.

D. G. Corr was with the Department of Electrical Engineering, University College, London, England. He is now with the Department of Electrical Engineering, University of British Columbia, Vancouver, B. C., Canada.

J. B. Davies was with the Department of Electrical Engineering, University College, London, England. He is now a Visiting Scientist, Electromagnetics Division, National Bureau of Standards, Boulder, Colo.

I. Introduction

IN MODERN microwave devices the integrated circuit is a fundamental component, and microstrip is an essential part of such circuits [1], [2]. Many articles have appeared giving design data for single microstrip [3]–[7], and for pairs of coupled strips [8], but common to all but a few of these publications is the assumption that the fundamental mode of propagation may be approximated by TEM mode propagation (the quasi-static approximation). Because microstrip is a device which contains two different dielectric media, the mode supported can never be TEM (except for dc operation), and in general a hybrid mode propagates. Design based on the quasi-static approximation has often been found to be adequate for the fundamental mode when considering operation below about 4 GHz with low permittivity substrates (κ below 6). However, recent developments require the operation of micro-

strip at higher frequencies [2], [9], [10], and the use of high permittivity substrates. For optimal design of microstrip devices, it is essential to have accurate information on the characteristics of the modes supported. The quasi-static approximation inherently cannot give information on dispersion or on the propagation of modes other than the fundamental.

An analysis is sought with the following objectives.

1) To deal with the true hybrid-mode nature of all microstrip modes. Information on dispersion and the field components is to be obtained for the dominant and higher order modes.

2) To consider microstrip within a conducting box (to give information on the effect of the enclosure that is necessary in practice).

3) Again, for realistic reasons, it must be possible for the enclosing conductor dimensions to be large compared with the microstrip conductor width and substrate thickness.

4) The method used should be sufficiently general to allow solutions to be obtained for single and coupled microstrip, and for related problems, such as slotline [2] and coplanar waveguide [2].

5) The analysis should be "exact in the limit" and not include avoidable approximations, so that accuracy is limited only by computer power. The only basic approximations conceded are the perfect geometry, the loss-free dielectric, and the infinite conductivity of the conductors.

Recently a number of papers [11]–[15] have appeared, dealing with the dispersive and hybrid-mode nature of microstrip. However, none of these meets all the above five objectives which are considered desirable for an understanding of microstrip structures.

The theory of Denlinger [13] does not consider the desirable objectives 2) and 5) above. He deals with the idealized structure of the open microstrip, and therefore cannot give information on the effects of the normal practice of enclosing the microstrip. His analysis includes the basic approximation of assuming a current distribution equal to that of quasi-TEM conditions.

The approaches of Daly [14] and Gopinath and Hornsby [11] have similar aims to those of this paper, but they seriously fall short of objective 3) above. Special attention has been taken in this work to consider objective 3) in the belief that otherwise one cannot study realistic geometries.

Mittra and Itoh [12] transform the conventional "mode-matching" method via the singular integral equation approach to give a determinantal equation that is more rapidly convergent than conventional mode matching. This is undoubtedly a powerful technique, but there are problems of slower convergence when analyzing structures with realistic (large) sized conducting boxes and when analyzing fast waves.

Zysman and Varon [15] give no details of how they solve their system of coupled integral equations, and make it virtually impossible to comment on their approach except to say that it would need modification to meet the objectives 2) and 4).

All the objectives 1) to 5) have been met in the method to be described. By the use of finite difference methods this work gives dispersion characteristics for several of the lowest order propagating modes in both single and coupled microstrip lines. For the investigation of structures with realistic dimensions by finite difference methods, it is thought to be essential to use the variational method described.

Two distinct advantages of the approach in this paper are a) the ability to deal equally with single microstrip, a pair of coupled strips, thick strips, overlay couplers [16], slot line [2], [17], or indeed any reasonable set of conductors and dielectric within a conducting box, and b) the use of an algorithm that finds the eigenvalues automatically and categorically for any given structure and phase velocity.

A brief outline of the work described in this paper has been given in [18].

II. Formulation of the Electromagnetic Field Problem for Microstrip

A microstrip line is considered to be symmetrically enclosed by a rectangular conducting box (Fig. 1). Although single microstrip lines are described, the procedure for coupled lines and other structures is very similar. The strips may have finite thickness, however, results are given only for strips of negligible thickness. The dielectric substrate is assumed to be homogeneous and isotropic. Propagation takes place in the z direction with a z dependence of $\exp(-j\beta z)$. Since the four transverse field components H_x, H_y, E_x, and E_y may be written in terms of E_z and H_z, then it is sufficient to solve the Helmholtz equations:

$$\nabla_t^2 H_z + k^2 H_z = 0 \tag{1}$$

$$\nabla_t^2 E_z + k^2 E_z = 0 \tag{2}$$

where

$$\nabla_t^2 = \frac{\partial^2}{\partial x^2} + \frac{\partial^2}{\partial y^2}$$

and

$$k^2 = \omega^2 \mu\epsilon - \beta^2$$

subject to the boundary conditions:

$$E_z = 0 \quad \frac{\partial H_z}{\partial n} = 0 \qquad \text{(at electric walls)}$$

$$\frac{\partial E_z}{\partial n} = 0 \quad H_z = 0 \qquad \text{(at magnetic walls)}$$

($\hat{n}$ = unit vector normal to the walls) and the continuity conditions (e.g., for an x-directed interface)

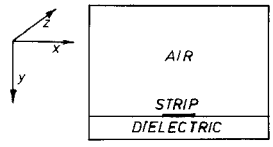

Fig. 1. Microstrip symmetrically enclosed by a waveguide.

$$\frac{\partial E_z}{\partial x}\beta\left[\frac{1}{k_A^2}-\frac{1}{k_D^2}\right] = \omega\mu_0\left[\frac{1}{k_D^2}\frac{\partial H_z}{\partial y}\bigg|_D - \frac{1}{k_A^2}\frac{\partial H_z}{\partial y}\bigg|_A\right] \quad (3)$$

$$\omega\mu\epsilon_0\frac{\partial H_z}{\partial x}\left[\frac{1}{k_A^2}-\frac{\kappa}{k_D^2}\right] = \beta\epsilon_0\left[\frac{1}{k_A^2}\frac{\partial E_z}{\partial y}\bigg|_A - \frac{\kappa}{k_D^2}\frac{\partial E_z}{\partial y}\bigg|_D\right] \quad (4)$$

where the subscripts A and D refer to the values in air and dielectric, respectively, and

$$k_A^2 \equiv k_0^2 = \omega^2\mu_0\epsilon_0 - \beta^2$$

and

$$k_D^2 = \omega^2\mu_0\epsilon_0\kappa - \beta^2.$$

In the way described it is possible to formulate the problem in terms of E_z and H_z. It is also possible that other pairs of field components may be used to describe the problem, such as the transverse electric or magnetic field components, and such alternatives have been considered [26], [27]. However, for reasons given in [26], the longitudinal field formulation is found most suitable.

The eigenvalues of the Helmholtz equations k_0^2 and k_D^2 are related according to the phase velocity v_pc (where v_p is the relative phase velocity and c the velocity of light):

$$\tau \equiv \frac{k_0^2}{k_D^2} = \frac{\omega^2\mu_0\epsilon_0 - \beta^2}{\omega^2\mu_0\epsilon_0\kappa - \beta^2} = \frac{1 - 1/v_p^2}{\kappa - 1/v_p^2}. \quad (5)$$

The range of solutions of the wave equation as a function of τ are shown in Fig. 2. There are two regions corresponding to propagating hybrid modes; these are termed the slow and fast wave regions, corresponding to propagation with $1/\sqrt{\kappa} < v_p < 1$ and $v_p \geq 1$, respectively. The fundamental mode is distinguished as that mode whose phase velocity tends to the static value as the frequency of operation tends to zero; consequently, the slow wave region is of particular interest. Unlike other sectors of the diagram, the slow-wave region is not uniquely defined by τ. When τ is negative, both slow-wave and transient-wave solutions are possible, corresponding to negative and positive values of k_0, respectively. In Section IV this will be seen to cause the matrix eigenvalue equation for the problem to be indefinite.

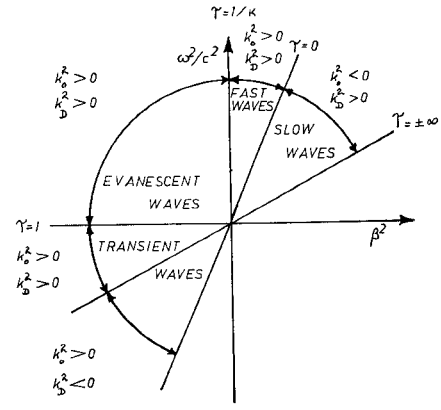

Fig. 2. Classification of hybrid mode solutions ω^2/c^2 versus β^2.

III. Derivation of the Finite Difference Equations

For the method of finite differences, the continuous fields are replaced by discretized field values. Normally, the partial differential equations governing the system are approximated by the direct use of Taylor's theorem resulting in a matrix eigenvalue equation [19]–[21]. Two considerations make this approach undesirable. First, the necessity for the use of efficient methods of solving the matrix eigenvalue equation. Second, the use of a graded finite difference mesh, which is required for the investigation of structures with realistic dimensions.

In general, the most efficient methods of solution are available for symmetric matrix eigenvalue problems [22]. When a graded mesh is used, the matrix of finite difference coefficients will be unsymmetric if obtained by the direct use of Taylor's theorem. A symmetric matrix can be obtained by the use of the variational method [20], [21], the method being applicable for self-adjoint systems. As well as always producing a symmetric matrix, this method has the advantage that certain boundary and interface conditions appear as "natural" boundary and interface conditions, and consequently do not require any special treatment.

The requirement that the mesh must be graded is to permit the investigation of structures with realistic dimensions, where the enclosing box is large compared to the strip width and substrate thickness. If a uniform mesh were used, then in order that the mesh be sufficiently fine for the strip to be adequately represented, the total number of mesh points has to be extremely large. The order of the finite difference matrix is directly proportional to the number of mesh points used, and in practice, storage requirements and speed of solution set an upper limit on the number of mesh points that may be used. However, the matrix order can be reduced and good accuracy still obtained by the use of a graded mesh. A fine mesh is then used only in regions where the fields vary most rapidly (i.e., in the vicinity of the strip, and the air–dielectric interface). Computing times and storage

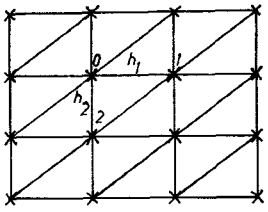

Fig. 3. Typical region within finite difference mesh.

can be reduced by factors of at least 100 and 10, respectively, by this graded mesh facility.

The derivation of the finite difference equations proceeds from the variational expression for an inhomogeneously filled structure. This is obtained directly from Maxwell's curl equations and has been given by Berk [23]. In terms of the longitudinal field components, we have

$$\iint \left[\frac{1}{k^2}(\omega\epsilon E_z \nabla_t^2 E_z + \omega\mu H_z \nabla_t^2 H_z) + \omega\epsilon E_z^2 + \omega\mu H_z^2\right] dS = 0. \quad (6)$$

By application of the divergence theorem, this may be put in a form which does not involve derivatives higher than the first order (which is required for the finite difference method to be used):

$$J = \iint \left[\left(\frac{\beta c}{\omega}\right)^2 \tau_r \kappa_r |\nabla_t \psi|^2 + \tau_r |\nabla_t \phi|^2 + 2\left(\frac{\beta c}{\omega}\right)^2 \tau_r \left(\frac{\partial \psi}{\partial x}\frac{\partial \phi}{\partial y} - \frac{\partial \phi}{\partial x}\frac{\partial \psi}{\partial y}\right) - k_0^2\left[\phi^2 + \left(\frac{\beta c}{\omega}\right)^2 \kappa_r \psi^2\right]\right] dS \quad (7)$$

where

$$\phi = H_z \quad \text{and} \quad \psi = \frac{\omega\epsilon_0}{\beta} E_z$$

$$\tau_r = k_0^2/(\omega^2\mu_0\epsilon_0\kappa_r - \beta^2)$$

$$\kappa_r = \begin{cases} 1, & \text{in air} \\ \kappa, & \text{in dielectric.} \end{cases}$$

J can be shown to be stationary in the normal way [23], [24].

For simplicity, the finite difference mesh is taken to have rectangular pitch, and is so arranged that mesh points lie exactly on the boundaries, the strip edge, and the interface. Each mesh point specifies a value for both ϕ and ψ, except at the boundaries where either ϕ and/or ψ may be zero.

Consider an elemental region in the difference mesh such as that described by 3 points (Fig. 3, putting $h_1 = h_2 = h$). The surface integral of (7) over this region may be approximated by using forward or backward difference formulas [20] to replace the first derivatives, e.g.,

$$\iint_\Delta |\nabla_t \phi|^2 \, dS \simeq \left[\left(\frac{\phi_1 - \phi_0}{h}\right)^2 + \left(\frac{\phi_2 - \phi_0}{h}\right)^2\right]\frac{h^2}{2}. \quad (8)$$

There is considerable freedom in the choice of approximations for terms in (7) such as $\iint \phi^2 \, dS$. Two possibilities are

$$\iint_\Delta \phi^2 \, dS \simeq \frac{1}{3}(\phi_0^2 + \phi_1^2 + \phi_2^2)\frac{h^2}{2} \quad (9)$$

or

$$\iint_\Delta \phi^2 \, dS \simeq \frac{1}{6}(\phi_0^2 + \phi_1^2 + \phi_2^2 + \phi_0\phi_1 + \phi_0\phi_2 + \phi_1\phi_2)\frac{h^2}{2}. \quad (10)$$

Equation (10) is consistent with linear in interpolation of ϕ over the region, and is the basis of methods known as finite elements [14]. Methods which use approximations of the type (9) are known as finite difference methods. Thus by the use of approximations of the form (8) and (9) or (8) and (10), it is possible to arrive at an approximation for the contribution from the elementary triangular region of Fig. 3 to the integral of (7). The surface integral J of (7) is then computed as the sum of approximations of each elemental region in the structure. The stationary property of J is utilized by differentiating in turn with respect to each of the variables $\phi_1, \phi_2, \cdots, \phi_i, \psi_1, \psi_2, \cdots, \psi_i$. In this way N linear equations are derived for the system where N is the total number of variables ϕ_i and ψ_i. Details on this are given in Appendix I for the finite difference type of approximation. In matrix notation, the following eigenvalue equation results:

$$Ax = \lambda x$$

by using approximations of the type (9), and

$$Ax = \lambda Bx$$

by using approximations of the type (10). Matrices A and B are symmetric band-structured matrices. From considerations of the solution of these equations (Section IV), equations in standard form (11) have considerable advantages. It should be noted that (12) cannot [25] be reduced to the standard form of (11) without destroying the band structure and so increasing considerably the computer storage requirements.

A numerical comparison was made [26] of the finite difference and simple finite element methods as applied to the empty rectangular waveguide, and it was found that there are no advantages to be obtained by the use of the finite element method.

IV. Solution of the Matrix Eigenvalue Equations

The solution is sought of the matrix eigenvalue equation in standard form $Ax=\lambda x$, where A is a symmetric band-structured matrix [19]–[21] of order n and bandwidth $2m+1$. Typically, for the specific application to microstrip, $n=360$ and $m=44$. Since the eigenvalues λ may take on both positive and negative values in the region of interest ($\tau<0$), then the matrix eigenvalue equation is indefinite. The algorithms chosen were most suitable for a symmetric band structured matrix; they were as follows.

1) A is reduced to tridiagonal form [28].

2) The eigenvalues of a tridiagonal matrix are found by the method of bisection [29].

3) The eigenvector associated with a specific eigenvalue was found by the method of inverse iteration [22], [30].

By the use of methods 1) and 2), all the eigenvalues of A may be found. In practice, only the negative eigenvalues closest to zero are required, and typically, the lowest 8 were categorically determined. It is important to realize that by these methods, it is impossible to omit any solutions, and this is a very desirable feature of the method used in comparison with iterative methods. In general, iterative methods converge to the eigenvalue closest to a given estimate; in Appendix II it is shown that the eigenvalue spectrum is much more complicated than might first be thought, and especially for this reason the use of iterative methods can give very misleading results.

If the finite element formulation of the problem had been used, not only is the minimum storage requirement approximately doubled by the need to store two band matrices, but the only appropriate algorithm available [31] which preserves the band structure is an iterative method. This particular method could be used to determine all the eigenvalues required, but it would be prohibitively inefficient to do so. There is certainly no numerical advantage to be obtained by the use of the simple finite element method.

V. Results

Using the methods described, dispersion curves are obtained in the form of graphs of κ_{eff} against frequency, where $\kappa_{eff}=1/v_p^2$. Although the Brillouin diagram is a more usual display of this information, κ_{eff} is a more sensitive parameter, and its use is widespread in microstrip literature. In addition to dispersion curves, power density diagrams are given at a particular frequency for certain modes. These are determined by evaluating the field components for a particular eigenvalue, and computing the power flow [32] from

$$P \propto \iint \mathrm{Re}\,(\boldsymbol{E}\times\boldsymbol{H}^*)\cdot d\boldsymbol{S}. \tag{11}$$

The diagrams show contours of equal power levels given in decibels relative to the highest power level.

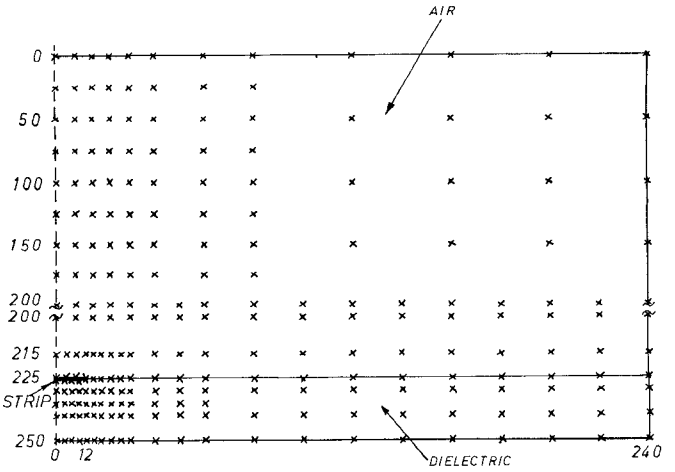

Fig. 4. Graded mesh used for single microstrip in a large box (half section shown). Note that the strip width equals the substrate thickness. Relative permittivity of substrate = 9.7. Scale: 1 unit = 0.002 in.

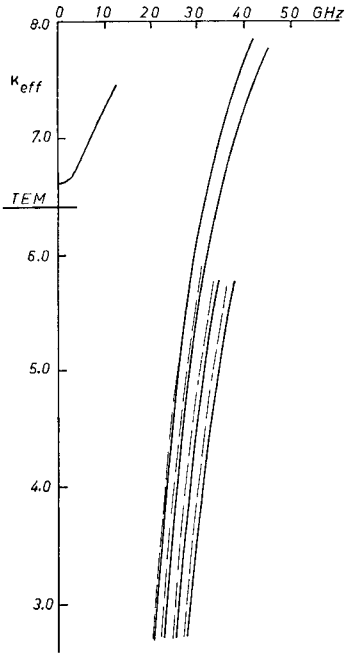

Fig. 5. Dispersion characteristics for the structure of Fig. 4. ———, modes with a magnetic wall symmetry plane; – – –, modes with an electric wall symmetry plane.

The results for two microstrip structures are presented: enclosed single microstrip and enclosed coupled microstrip lines.

Single microstrip

The configuration considered is shown in half section in Fig. 4. The crosses designate mesh point values; it should be noted that the vertical scale is discontinuous. The dispersion curve obtained for many of the propagating modes is shown in Fig. 5; this shows results for both electric and magnetic wall symmetry planes. The value of κ_{eff} for the structure is given for static (TEM) operation, derived by accurate finite difference solution of the two associated static problems [26]. It is seen that there is indeed one mode without a frequency cutoff, and this

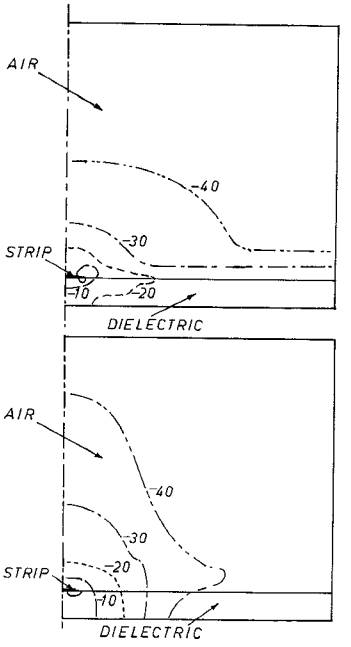

Fig. 6. Power flow diagrams for structure in Fig. 4 giving contours of equal power density in decibels relative to the highest contour. (a) Fundamental mode at frequency 1.9 GHz ($\kappa_{eff}=6.64$). (b) Static solution ($\kappa_{eff}=6.41$).

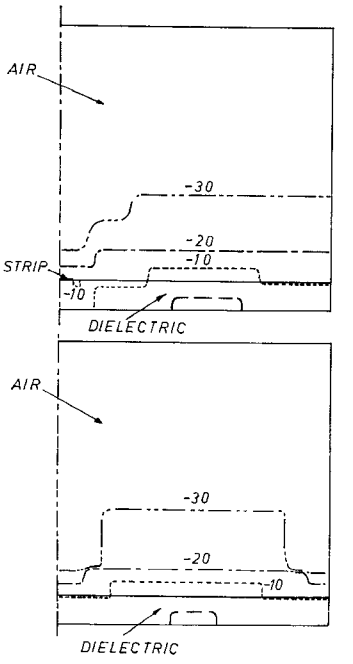

Fig. 7. (a) Power flow diagram for structure of Fig. 4 giving contours of equal power density in decibels relative to the highest contour. Higher order mode M_1 (see text) at frequency 22.9 GHz ($\kappa_{eff}=4.0$). (b) Power flow diagram for the LSM_{12} mode on the associated slab line for the structure of Fig. 4 at frequency 22.7 GHz ($\kappa_{eff}=4.0$).

is seen to become highly dispersive above 2 GHz. The difference between the static limiting value of κ_{eff} for this mode and the TEM value shown is due entirely to discretization errors [20] in the hybrid mode analysis. There are also seen to be a number of higher order modes which have a low-frequency cutoff; for reference these are designated according to their plane of symmetry E or M for electric and magnetic walls, respectively, and numbered in order of ascending cutoff frequency. Thus in this way, the higher order modes are specified by the letters E_1, M_1, E_2, M_2, E_3, M_3, etc., left to right on the dispersion curve. It is seen that the dispersion curves tend to group in pairs of modes with the same subscript, i.e., E_1 and M_1 mode dispersion curves are very close together.

Further information of the modes was found by examination of power density diagrams. Fig. 6 shows diagrams for both the fundamental mode and for the static case. It is seen that there is considerable similarity between the two diagrams, and at the frequency given, the power flow is mainly below the strip in the dielectric substrate region.

Because the microstrip occupies only a small fraction of the total dielectric surface in the structure considered, then slow wave propagation by the associated slab line structure is of considerable interest. Specifically, we can consider the structure formed by the removal of the microstrip. Propagation of LSM and LSE modes by slab line structures is, of course, well known [32]. The dispersion curves for these modes were compared with the higher order microstrip modes, and it was found that there was a very close correspondence in the curves for the LSM modes and the high-order microstrip modes. It was further found by the examination of the power density diagrams that there was a very close similarity between the diagrams for the modes M_1 and LSM_{12}, and between M_2 and LSM_{14}; the diagrams for the former case are given in Fig. 7. The conclusions drawn about the higher order modes are given in the discussion for coupled strip below; however, it should be noted that apart from these modes, the device supports only one other type of mode, the fundamental mode for which κ_{eff} tends to the static value as $f\rightarrow 0$. The "surface-wave" modes reported by Daly [14] are considered in Appendix II and are shown to be a misinterpretation of results.

Coupled Strips

The coupled strip device is shown in half section in Fig. 8; it should be noticed that again the vertical scale is broken. The dispersion curves for the structure are shown in Fig. 9 together with the static case parameters. The two modes without a low-frequency cutoff value correspond to the "even" and "odd" modes; these have magnetic wall and electric wall symmetry, respectively. It is seen that the limiting values of κ_{eff} for these modes are in good agreement with the respective static values. A number of higher order modes exist, and

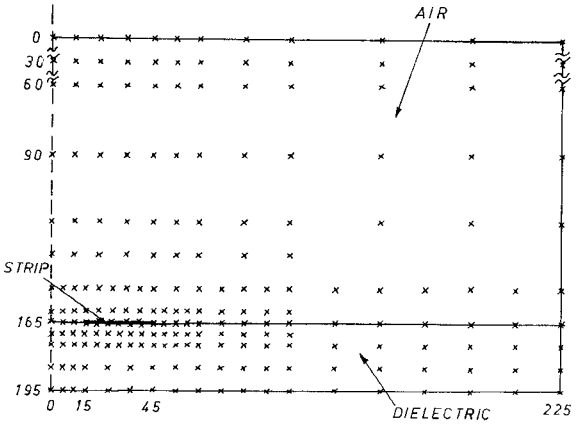

Fig. 8. Graded mesh used for coupled strips in large box (half section shown). Note that the strip width equals the substrate thickness. Relative permittivity = 9.7. Scale: 1 unit = 0.001 in.

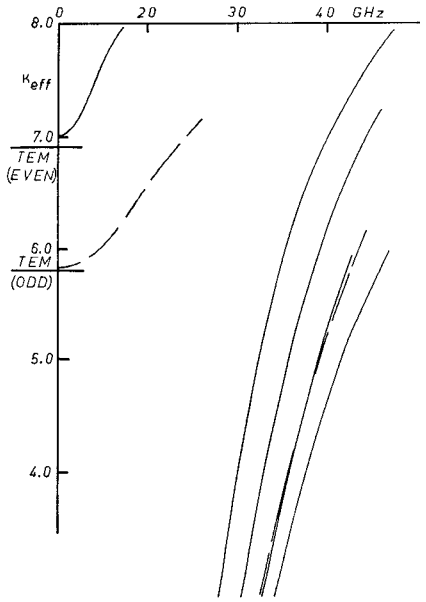

Fig. 9. Dispersion characteristics for the structure of Fig. 8. ———, modes with a magnetic wall symmetry plane; – – –, modes with an electric wall symmetry plane. Note that modes E_1 and M_1, E_2 and M_2, E_4 and M_4 are virtually coincident.

these are seen to be grouped in pairs in a manner similar to that noted above for single microstrip. Again, it was found that the dispersion curves for the LSM modes which propagate in the associated slab line structure were almost identical to those obtained for the high-order coupled strip modes. Examination of power density diagrams showed that the modes M_1 and E_1 are very similar to each other and to the LSM_{12} mode. It is concluded that because the plane of symmetry makes so little difference to the higher order modes with the same subscript, then these modes are strongly associated not with the strip, but with the dielectric–air interface between the strip edge and the outer side wall of the enclosure. In view of their close similarity to the LSM modes, they are best considered as distorted LSM modes. The specific type of mode correspondences are grouped below:

$$E_1 \quad M_1 \quad LSM_{12}$$

$$E_2 \quad M_2 \quad LSM_{14}.$$

Thus for enclosed microstrip devices, an approximate indication of the frequency when high-order modes will propagate is given by a simple calculation of the cutoff frequency of the LSM_{12} mode.

It should be noted that when the dimensions of the enclosing conducting box are just a few times the strip width (e.g., the case given in Appendix II), then the effect of the strip is to greatly perturb the slab line type modes, and the design indication given above ceases to be accurate.

VI. Conclusion

The specific conclusions of this work are as follows.

1) Theory and typical results are given for the numerical solution of a class of inhomogeneously filled waveguide problems with or without inner conductors.

2) Notable features of the approach are as follows.

a) A nonuniform mesh can be used to allow the investigation of realistic structures, and to make optimum use of the available computer capability.

b) Special attention has been given in the formulation in order to use matrix methods which allow categorical determination of the eigenvalues.

3) Results for the main objective of this work have been obtained for two realistic microstrip devices. Complete dispersion curves for these devices were obtained, and the following are shown.

a) The dominant mode in microstrip is dispersive, but in the zero frequency limit it can be identified with the static case. Similar results for the two dominant modes in coupled strip were also obtained.

b) There is a close relation between the higher order modes, and the LSM modes for the associated slab loaded waveguide. This suggests that a simple estimate of the frequency at which higher order modes will propagate may be obtained through consideration of the well-known (and easily calculated) LSM modes.

4) Attention is drawn to the physically spurious modes described in Appendix II. These modes are thought to be present in any finite difference or finite element formulation for inhomogeneous problems when slow wave solutions are sought.

5) The "surface wave" mode reported by Daly [14] is believed to be just one of the spurious modes mentioned in 4) above. All the features of the mode which he describes have characteristics of the spurious modes discussed in this work.

Appendix I

By dividing the structure into a number of elemental regions, then (7) may be approximated by $J \simeq \sum_j S_j$. Considering a particular triangular region as given in Fig. 3(a), by the use of finite difference approximations S_j may be obtained. By differentiation with respect to each of the mesh point variables, the following matrix equation results:

$$\begin{bmatrix} \frac{\partial S_j}{\partial \phi_0} \\ \frac{\partial S_j}{\partial \psi_0} \\ \frac{\partial S_j}{\partial \phi_1} \\ \frac{\partial S_j}{\partial \psi_1} \\ \frac{\partial S_j}{\partial \phi_2} \\ \frac{\partial S_j}{\partial \psi_2} \end{bmatrix} = \begin{bmatrix} \tau\left(\frac{h_2}{h_1}+\frac{h_1}{h_2}\right) & 0 & \frac{-\tau h_2}{h_1} & -W & \frac{-\tau h_1}{h_2} & W^* \\ 0 & P\left(\frac{h_2}{h_1}+\frac{h_1}{h_2}\right) & W & \frac{-Ph_2}{h_1} & -W^* & \frac{-Ph_1}{h_2} \\ \frac{-\tau h_2}{h_1} & W & \frac{\tau h_2}{h_1} & 0 & 0 & -W^* \\ -W & \frac{-Ph_2}{h_1} & 0 & \frac{Ph_2}{h_1} & W & 0 \\ \frac{-\tau h_1}{h_2} & -W^* & 0 & W & \frac{\tau h_1}{h_2} & 0 \\ W^* & \frac{-Ph_1}{h_2} & -W^* & 0 & 0 & \frac{Ph_1}{h_2} \end{bmatrix} \begin{bmatrix} \phi_0 \\ \psi_0 \\ \phi_1 \\ \psi_1 \\ \phi_2 \\ \psi_2 \end{bmatrix} - \frac{h_1 h_2 k_0^2}{3} \begin{bmatrix} 1 & & & & & \\ & P' & & & & \\ & & 1 & & & \\ & & & P' & & \\ & & & & 1 & \\ & & & & & P' \end{bmatrix} \begin{bmatrix} \phi_0 \\ \psi_0 \\ \phi_1 \\ \psi_1 \\ \phi_2 \\ \psi_2 \end{bmatrix}$$

where

$$P' = \left(\frac{\beta c}{\omega}\right)^2 \kappa \qquad P = \tau P'$$

and

$$W^* = W = \left(\frac{\beta c}{\omega}\right)^2 \tau$$

(but see text following).

It can be shown that for a graded mesh system, it is preferable to set $W = 0$ except when an air–dielectric interface bounds one side of the triangle; in this case the terms W indicated by an asterisk should be included. These terms are specified here for the case of an x-directed interface.

By repeated application of matrices of the form given above, and by utilizing the stationary property of (7), then N linear equations may be obtained for the system.

Appendix II

The mathematical formulation of the problem is such that for a particular structure, v_p $(= 1/\sqrt{\kappa_{\text{eff}}})$, is the only independent variable. By the use of the algorithms mentioned in Section IV, a number of solutions are found for the eigenvalue equation, each eigenvalue corresponding to a different frequency value for the same value of v_p. Such values are designated by "×" on Fig. 10. By taking a sufficient number of values of v_p, after careful consideration it is possible to connect the results uniquely by smooth curves. This can be done with confidence knowing that for a particular value of v_p all the solutions (for frequency) are obtained within the range plotted. This categorical evaluation of all eigenvalues within a given interval is a feature of the Sturm sequence properties [22], [29]. The resulting dispersion curves are seen to be unexpectedly complicated. However, the dispersion curves can be interpreted as a superimposition of two classes of results (Fig. 11). One class consists of the fundamental microstrip mode, which is noted to tend to the static value of κ_{eff} as $f \to 0$, and a number of higher order modes which have frequency cutoff. The other class consists of a large number of modes without a low-frequency cutoff; these are nonphysical modes which nevertheless satisfy the approximate mathematical formulation of the problem. The tessellated pattern of Fig. 10, with individual curves smoothly alternating between two intersecting classes of modes, is typical of a coupled mode system [33].

The cause of these spurious solutions is believed to be in the indefinite nature of the variational expression, (7). Similar extraneous solutions are reported by Harrington [34] that occur for an indefinite system but not for a definite system. The identification of the spurious mode class was made by investigation of slab-loaded waveguide structures. The modes which propagate on this type of structure are well known [32]; however using the formulation described, it was found that as well as these physical modes, spurious modes were also present of identical appearance to those in Fig. 11. It was found that the number of these modes was equal to the number of mesh points on the air–dielectric interface, and that each mode could be characterized by the number of changes of sign of the values of ϕ across the interface. Again, this number of spurious solutions agrees with Harrington's findings [34], where one free boundary point gave rise to one spurious solution, and two points to two spurious solutions. These modes were

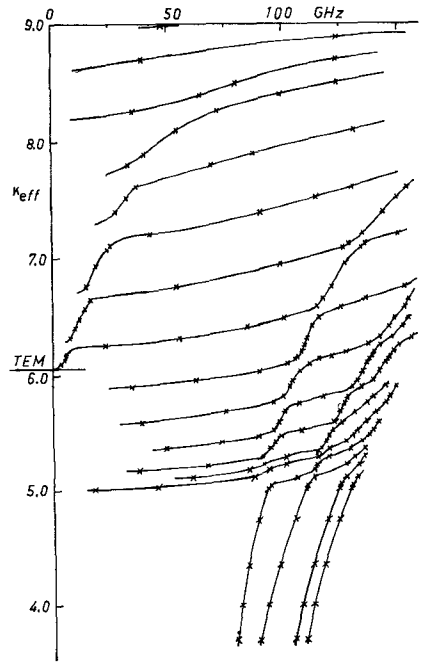

Fig. 10. Dispersion results computed for enclosed single microstrip. Strip width = 1.0 mm; substrate thickness = 0.5 mm; height of enclosure = 2.0 mm; width of enclosure = 3.5 mm; relative permittivity = 9.0.

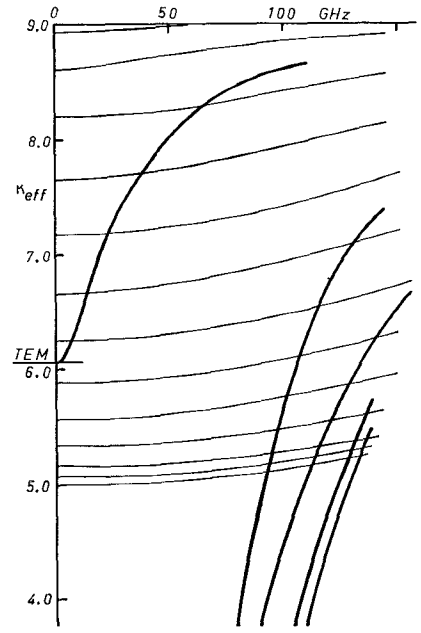

Fig. 11. Dispersion curve interpolated from results of Fig. 10. ———, spurious modes; ———, physical modes.

found to exist only in the range

$$\kappa < \kappa_{\text{eff}} < \frac{\kappa + 1}{2}.$$

Apart from the considerations given, it would be very difficult to account for these modes physically; their number, absence of low-frequency cutoff, and their rapid spatial dependence of field components along the dielectric–air interface all point to their being nonphysical.

The dispersion curves given in this paper (except Fig. 10) represent the interpolated curves derived from more complex curves, like Fig. 10, which contain the spurious mode solutions.

References

[1] M. V. Schneider, "Microstrip lines for microwave integrated circuits," *Bell Syst. Tech. J.*, vol. 48, pp. 1421–1444, May–June 1969.
[2] H. Sobol, "Applications of integrated circuit technology to microwave frequencies," *Proc. IEEE (Special Issue on Microwave Semiconductors)*, vol. 59, pp. 1200–1211, Aug. 1971.
[3] H. A. Wheeler, "Transmission-line properties of parallel strips separated by a dielectric sheet," *IEEE Trans. Microwave Theory Tech.*, vol. MTT-13, pp. 172–185, Mar. 1965.
[4] P. Silvester, "TEM wave properties of microstrip transmission lines," *Proc. Inst. Elec. Eng.*, vol. 115, pp. 43–48, Jan. 1968.
[5] E. Yamashita and R. Mittra, "Variational method for the analysis of microstrip lines," *IEEE Trans. Microwave Theory Tech.*, vol. MTT-16, pp. 251–256, Apr. 1968.
[6] S. V. Judd, I. Whiteley, R. J. Clowes, and D. C. Rickard, "An analytical method for calculating microstrip transmission line parameters," *IEEE Trans. Microwave Theory Tech.*, vol. MTT-18, pp. 78–87, Feb. 1970.
[7] H. E. Stinehelfer, Sr., "An accurate calculation of uniform microstrip transmission lines," *IEEE Trans. Microwave Theory Tech.*, vol. MTT-16, pp. 439–444, July 1968.
[8] T. G. Bryant and J. A. Weiss, "Parameters of microstrip transmission lines and of coupled pairs of microstrip lines," *IEEE Trans. Microwave Theory Tech.*, vol. MTT-16, pp. 1021–1027, Dec. 1968.
[9] K. C. Wolters and P. L. Clar, "Microstrip transmission lines on high dielectric constant substrates for hybrid microwave integrated circuits," in *1967 G-MTT Symp. Dig.*, pp. 129–131, May 1967.
[10] G. D. Verdlin, "High dielectric substrates for microwave hybrid integrated circuitry," in *1967 G-MTT Symp. Dig.*, pp. 125–128, May 1967.
[11] J. S. Hornsby and A. Gopinath, "Numerical analysis of the dielectric-loaded waveguide with a microstrip line—Finite-difference methods," *IEEE Trans. Microwave Theory Tech.*, vol. MTT-17, pp. 684–690, Sept. 1969.
[12] R. Mittra and T. Itoh, "A new technique for the analysis of the dispersion characteristics of microstrip lines," *IEEE Trans. Microwave Theory Tech.*, vol. MTT-19, pp. 47–56, Jan. 1971.
[13] E. J. Denlinger, "A frequency dependent solution for microstrip transmission lines," *IEEE Trans. Microwave Theory Tech.*, vol. MTT-19, pp. 30–39, Jan. 1971.
[14] P. Daly, "Hybrid-mode analysis of microstrip by finite-element methods," *IEEE Trans. Microwave Theory Tech.*, vol. MTT-19, pp. 19–25, Jan. 1971.
[15] G. I. Zysman and D. Varon, "Wave propagation in microstrip transmission lines," in *1969 G-MTT Symp. Dig.*, pp. 3–9, May 1969.
[16] K. C. Wolters, P. L. Clar, and C. W. Stiles, "Analysis and experimental evaluation of distributed overlay structures in microwave integrated circuits," in *1968 G-MTT Symp. Dig.*, pp. 123–130, May 1968.
[17] E. A. Mariani, C. P. Heinzman, J. P. Agrios, and S. B. Cohn, "Slot line characteristics," *IEEE Trans. Microwave Theory Tech.*, vol. MTT-17, pp. 1091–1096, Dec. 1969.
[18] J. B. Davies and D. G. Corr, "Computer analysis of the fundamental and higher-order modes in single and coupled microstrip," *Electron. Lett.*, vol. 6, pp. 806–808, Dec. 1970.
[19] R. S. Varga, *Matrix Iterative Analysis*. Englewood Cliffs, N. J.: Prentice-Hall, 1962.
[20] G. E. Forsythe and W. R. Wasow, *Finite-Difference Methods for Partial Differential Equations*. New York: Wiley, 1965.
[21] E. L. Wachspress, *Iterative Solution of Elliptic Systems and Applications to the Neutron Diffusion Equations of Reactor Physics*. Englewood Cliffs, N. J.: Prentice-Hall, 1965.
[22] J. H. Wilkinson, *The Algebraic Eigenvalue Problem*. London, England: Clarendon, 1965.
[23] A. D. Berk, "Variational principles for electromagnetic resonators and waveguides," *IRE Trans. Antennas Propagat.*, vol. AP-4, pp. 104–111, Apr. 1956.

[24] S. Ahmed, "Finite-element method for waveguide problems," *Electron. Lett.*, vol. 4, pp. 387–389, Sept. 1968.
[25] R. S. Martin and J. H. Wilkinson, "Reduction of the symmetric eigenproblem $Ax=\lambda Bx$ and related problems to standard form," *Numerische Mathematik*, vol. 11, pp. 99–110, 1968.
[26] D. G. Corr, "Finite difference analysis of hybrid modes in microstrip structures," Ph.D. dissertation, University of London, London, England, Aug. 1970.
[27] D. Gelder, "Numerical determination of microstrip properties using the transverse field components," *Proc. Inst. Elec. Eng.*, vol. 117, pp. 699–703, Apr. 1970.
[28] H. R. Schwartz, "Tridiagonalization of a symmetric band matrix," *Numerische Mathematik*, vol. 12, pp. 231–241, 1968.
[29] W. Barth, R. S. Martin, and J. H. Wilkinson, "Calculation of the eigenvalues of a symmetric tridiagonal matrix by the method of bisection," *Numerische Mathematik*, vol. 9, pp. 336–393, 1967.
[30] J. H. Wilkinson, "Calculation of the eigenvectors of a symmetric tridiagonal matrix by inverse interation," *Numerische Mathematik*, vol. 4, pp. 368–376, 1962.
[31] G. Peters and J. H. Wilkinson, "Eigenvalues of $Ax=\lambda Bx$ with band symmetric A and B," *Comput. J.*, vol. 12, pp. 398–404, 1969.
[32] R. E. Collin, *Field Theory of Guided Waves*. New York: McGraw-Hill, 1960.
[33] P. M. Morse and H. Feshbach, *Methods of Theoretical Physics*, vol. 2. New York: McGraw-Hill, 1953, p. 1477.
[34] R. F. Harrington, *Field Computation by Moment Methods*. New York: Macmillan, 1968, pp. 147–150.

Frequency-Dependent Characteristics of Microstrip Transmission Lines

MARK K. KRAGE AND GEORGE I. HADDAD

***Abstract*—A method for determining the frequency-dependent characteristics of both single and coupled lines in shielded microstrip is presented. Numerical results are given for a variety of dielectric configurations and the effects of geometry on the dispersion characteristics are examined in detail. Of particular interest are the characteristics of coupled lines on compensated dielectric structures, i.e., structures that are capable of achieving equal even- and odd-mode phase velocities, and the effects of dispersion on the directivity characteristics of such lines are discussed. In addition, the variation of impedance as a function of frequency, where the impedance is defined as the ratio of the power to the square of the longitudinal current, is presented for representative cases of single and coupled lines.**

I. Introduction

FOR sufficiently low frequencies the quasi-TEM theory can be employed to obtain the characteristics of microstrip lines and, using this approximation, extensive design data have been calculated for both single and coupled lines [1]–[3]. When the wavelength in a microstrip line becomes comparable to the transverse dimensions of the line the deviation from quasi-TEM behavior becomes significant and higher order modes of propagation become possible. Recently, several authors [4]–[10] have advanced methods for calculating the frequency-dependent characteristics of microstrip lines, but only limited numerical results have been presented for both open and shielded microstrip configurations. Most authors have confined their attention to the dominant mode characteristics of single lines, but Denlinger [9] and Gelder [10] have considered the characteristics of a pair of coupled lines and Mittra and Itoh [7] and Pregla and Schlosser [11] have considered higher order modes in a shielded structure.

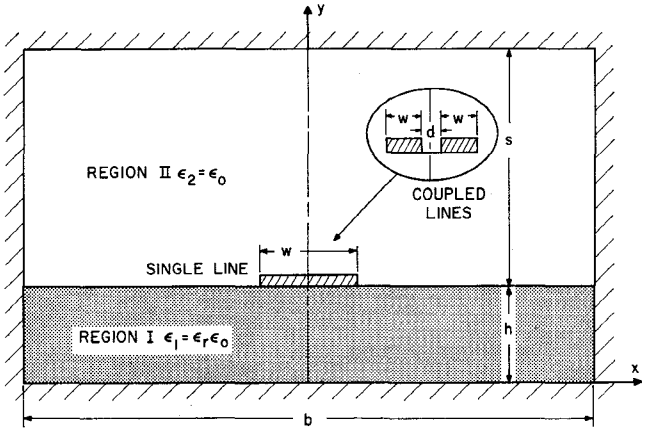

Fig. 1. Shielded microstrip geometry.

In this paper a method is presented for calculating the frequency-dependent characteristics of shielded microstrip lines, and the effects of geometry on the dispersion characteristics of single and coupled lines are considered in detail. Although the analysis will be carried out only for the configuration of Fig. 1, results will be presented for the modified configurations of Figs. 2 and 3, as well as for the geometry of Fig. 1. It was demonstrated in a previous paper [3] that coupled lines on the modified geometries can achieve equal even- and odd-mode phase velocities and are therefore capable of achieving high

Manuscript received January 31, 1972; revised May 8, 1972. This work was supported by a grant from Omni Spectra, Inc., Farmington, Mich.

M. K. Krage was with the Electron Physics Laboratory, Department of Electrical and Computer Engineering, University of Michigan, Ann Arbor, Mich. 48104. He is now with the General Motors Research Laboratories, Warren, Mich.

G. I. Haddad is with the Electron Physics Laboratory, Department of Electrical and Computer Engineering, University of Michigan, Ann Arbor, Mich. 48104.